# Solution of DC Railway Traction Power Flow Systems Including Limited Network Receptivity

Rabih A. Jabr, *Fellow, IEEE*, and Izudin Džafić, *Senior Member, IEEE*

***Abstract*—The voltage solution of DC railway traction power networks is classically obtained via the current injection (CI) method, which is based on solving a sequence of nodal voltage equations. Specialized techniques, which build on the CI method, have been proposed for simulating limited network receptivity due to voltage rise constraints and nonreversible substations. These techniques may require a multitude of power reduction steps for modeling the local controller operation of trains in regenerative braking mode, and they consequently lead to a large computational effort. This paper proposes a sensitivity-based approach for computing the regenerative train power that can be returned to the network without causing over voltage. In the case of nonreceptive substations, each regenerating train is switched to a voltage–current source model and the CI method is used to further adjust the power that can be received by the network; a two-phase approach is used to compute the regenerative train resistance without recourse to iterations. The proposed method is tested on network models with branched lines, detailed return circuits, and having up to 144 trains. The computational performance comparisons show that the proposed method for simulating local controllers can be significantly faster than the classical power reduction method.**

***Index Terms*—Load flow analysis, load flow control, power control, traction power supplies, voltage control.**

## NOMENCLATURE

| | |
|---|---|
| $cj$ | Index of catenary node with regenerating train connection and voltage higher than the limit. |
| $G_{gk}$ | Element in row $g$ and column $k$ of the modified conductance matrix. |
| $[H]$ | Sensitivity matrix. |
| $I_{gk}$ | Current directed from node $g$ to node $k$. |
| $I_k$ | Current injection at node $k$. |
| $m$ | Iteration counter in the CI method. |
| $N$ | Total number of nodes. |
| $P_{Tk}$ | Train power defined according to the active sign convention. |
| $R_k$ | Resistance of the regenerative train in the voltage-current source model at catenary node $k$. |
| $R_{gk}$ | Element in row $g$ and column $k$ of the modified resistance matrix. |
| $V_k$ | Voltage at node $k$. |
| $V_j^{\max}$ | Maximum permissible voltage at node $j$. |
| $V_s$ | Substation voltage. |
| $\Delta P_{Tj}$ | Computed change in power injection at catenary node $j$. |
| $\Delta V_j$ | Deviation between the maximum voltage magnitude and its computed value at catenary node $j$. |

Manuscript received November 20, 2016; revised February 26, 2017; accepted March 24, 2017. Date of publication March 28, 2017; date of current version December 20, 2017. Paper no. TPWRS-01736-2016. *(Corresponding author: Rabih A. Jabr.)*

R. A. Jabr is with the Department of Electrical & Computer Engineering, American University of Beirut, Beirut 1107 2020, Lebanon (e-mail: rabih.jabr@aub.edu.lb).

I. Džafić is with the International University of Sarajevo, Sarajevo 71210, Bosnia (e-mail: idzafic@ieee.org).

Digital Object Identifier 10.1109/TPWRS.2017.2688338

## I. INTRODUCTION

DESIGNING a DC rail traction power system or modifying an existing one is achieved by computer-aided techniques based on simulation. Traction simulators are employed to establish equipment ratings, to assess train regeneration effects, and to verify that catenary voltages remain within permissible limits and that rail potential and earth leakage currents are kept according to specifications for safety and interference mitigation [1], [2]. Traction simulators are based on power flow calculations carried out at different time instants sampled from the study horizon; the locations and power demands of the vehicles vary over the study period, and each instant has the trains represented using the stationary equivalents for moving vehicular loads [3]. A typical simulation study may require hundreds of sampled instants and consequently a significant computational effort; this effort increases with the sampling rate employed over the study horizon [4]. The computational effort is further exacerbated with the simulation of regenerative train breaking and nonreversible substations, as this requires additional power flow iterations for modeling the behavior of the train local controllers [5]. This paper proposes the use of a sensitivity approach as a means to enhance computational performance when modeling local controllers in DC traction power flow.

### A. Related Work

Transport via railways is increasing, thus creating a need for techniques to study the expansion planning and investment in railway power systems [6], [7]. DC traction power flow is employed in studies for supplying railway traction power equipment or for supporting tendering and contracting activities [8]. The simulators used by the industrial companies commonly employ the conductance matrix iterative approach with the trains represented either as conductances or as current sources [1], [2], [8]; a comparison reported in [5] showed that the current source train model is superior in terms of convergence speed. The conductance matrix iterative approach using the current source train model is known as the current injection (CI) power flow. The conductance matrix that arises in the CI method is a

0885-8950 © 2017 IEEE. Personal use is permitted, but republication/redistribution requires IEEE permission.
See http://www.ieee.org/publications_standards/publications/rights/index.html for more information.

Authorized licensed use limited to: American University of Beirut. Downloaded on May 08,2024 at 05:24:30 UTC from IEEE Xplore. Restrictions apply.

sparse representation of the nodal voltage equations for a ladder type network; this matrix is large because it includes rail nodes that turn out in finite cell modeling of return circuits [9], but typically more than 80 percent of its elements are zeros [10]. The solution of the nodal equations at each iteration of the CI method can be carried out using direct matrix factorization methods [10], or indirect methods such as incomplete Cholesky conjugate gradient [11]. Other techniques for traction power flow include Newton-Raphson type methods [4], optimal power flow solutions [12], and the forward-backward sweep power flow [13]. The DC traction power flow has been also extended to model the AC distribution network [12], [14], [15], and onboard train storage [16], [17]. The simulation of trains that utilize combined regenerative and rheostatic braking requires the modeling of local controllers that limit the maximum pantograph voltage; a survey of the related literature [1], [2], [4], [5], [10]–[17] shows that this type of control has been reported in [5], [12], [13], [16]. The local voltage regulation employed during braking so that the catenary voltage does not exceed a prescribed limit is referred to as squeeze control [13]; squeeze control reduces the regenerated power that is returned to the network by diverting part of it to the rheostatic braking system, with the aim of bringing the catenary voltage within its preset limit. However, limited network receptivity is not only attributed to voltage rise limitations, but also to nonreversible substations; in this respect, only [5] simulates non-receptive substations while [12], [13], [16] all consider DC transit systems that are fitted with inverting substations, as described in [18]–[20]. Both the CI method [5] and the forward-backward sweep technique [13] have been also investigated for the power flow solution of AC distribution networks [21], [22], and the superiority of the CI method for handling meshes is well understood.

### B. Technical Contribution

This paper builds on the CI method and the associated techniques [5] to simulate the local control of the regenerative chopper in blended regenerative/rheostatic braking so as to handle voltage rise constraints and non-receptive supplies. It presents two contributions that aim to improve the computational performance of the power flow as compared to [5]. These contributions are:

1) a sensitivity method to handle local controllers that is competitive with the power reduction and balance method in [5]. A closed-form solution for the elements of the sensitivity matrix is derived.
2) a hybrid voltage-current source model to reset the pantograph voltage of regenerating trains when substations are reverse biased. As compared to [5], a two-phase simulation approach is proposed for computing the regenerative train resistance without iteration; this extends the voltage source model in [5] to effectively handle non-receptive substations in networks with detailed models of return circuits.

This study also brings attention to the analysis of this special type of power networks with moving vehicular loads, at the time the electrification of railway systems is becoming increasingly important [6], [7].

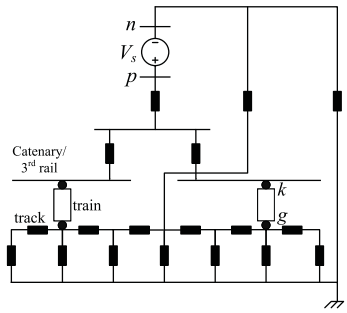


Fig. 1. DC traction power network.

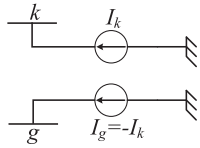


Fig. 2. Current source train model.

### C. Paper Structure

The rest of this paper is organized as follows. Section II presents the formulation of the DC traction power flow problem and its solution using the CI method. The main contributions of the paper, i.e. the simulation of local controllers and the two phase approach for handling non-receptive substations, are described in Section III. Section IV includes numerical results on four DC traction networks with branched lines, and a comparative analysis with the approach in [5]. The paper is concluded in Section V.

## II. DC Railway Traction Power Flow Solution

Consider a DC railway traction network having $N$ nodes, $N_S$ substations, and $N_T$ trains. The electrical performance of the network can be obtained from a sequence of power flow solutions representing different time instants over the study horizon, with the trains frozen in time for each instant; this approach is referred to as the stationary equivalent method for moving loads [3]. Fig. 1 shows a portion of a DC railway traction system forming a ladder type network. Each train is connected electrically between the catenary (or third rail) and the track, whose running rails are used for traction current return. The earth leakage currents are modeled to flow through a ladder network composed of finite cells, each represented by an equivalent $\pi$-circuit [9]. The substation is connected between the positive busbar $p$ and the negative busbar $n$, which itself is grounded and also connected to the track for current return. Consider a train connected between a catenary node $k$ and track node $g$; the train power is related to the node voltages and the current $I_{gk}$ in the train via:

$$P_{Tk} = (V_k - V_g)I_{gk} \tag{1}$$

where $P_{Tk}$ is defined according to the active sign convention, i.e. $P_{Tk} < 0$ indicates that the train is absorbing power in the motoring mode and $P_{Tk} > 0$ is for the train supplying power in the regenerative braking mode. Fig. 2 shows that the train can

Authorized licensed use limited to: American University of Beirut. Downloaded on May 08,2024 at 05:24:30 UTC from IEEE Xplore. Restrictions apply.

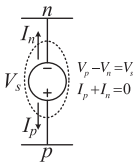


Fig. 3. Super-node substation model.

be represented via two current source injections, the first at the catenary node $k$ and the second at the track node $g$:

$$I_k = I_{gk} = \frac{P_{Tk}}{V_k - V_g} \tag{2}$$

$$I_g = -I_{gk} = \frac{-P_{Tk}}{V_k - V_g} \tag{3}$$

A substation connected between the positive busbar $p$ and the negative busbar $n$ stipulates two equations:

$$V_p - V_n = V_s \tag{4}$$

$$I_p + I_n = 0 \tag{5}$$

where (5) is effectively a super-node equation in which the sum of current injections into nodes $p$ and $n$ is set to zero; this is depicted in Fig. 3. The network nodal voltages are related to the nodal injection currents through the modified conductance matrix [23]:

$$\begin{bmatrix} 1 & -1 & 0 & \cdots & \cdots & 0 \\ \vdots & \ddots & \vdots & \vdots & \ddots & \vdots \\ G_{k1} & \cdots & G_{kk} & G_{kg} & \cdots & G_{kN} \\ G_{g1} & \cdots & G_{gk} & G_{gg} & \cdots & G_{gN} \\ \vdots & \ddots & \vdots & \vdots & \ddots & \vdots \\ G_{N1} & \cdots & G_{Nk} & G_{Ng} & \cdots & G_{NN} \end{bmatrix} \begin{bmatrix} V_1 \\ \vdots \\ V_k \\ V_g \\ \vdots \\ V_N \end{bmatrix} = \begin{bmatrix} V_s \\ \vdots \\ I_k \\ I_g \\ \vdots \\ 0 \end{bmatrix} \tag{6}$$

The network voltage solution is obtained by iterating the current injection values (2)–(3) with voltage solution from the network (6), until the scheduled train power values are satisfied within tolerance. The iterative procedure is known as the current injection power flow; it consists of the following steps:

*Step 1:* (Initialization) Form the $[G]$ matrix on the left hand side of (6) and factorize it using optimally-ordered sparse LU decomposition. Initialize all catenary node voltages to $V_s$, all track node voltages to zero, and the iteration counter $m = 0$.

*Step 2:* (Current Update) Increment the iteration counter $m$ by 1 and compute the node current injection vector $\left[I^{(m)}\right]$:

$$I_k^{(m)} = -I_g^{(m)} = \frac{P_{Tk}}{V_k^{(m-1)} - V_g^{(m-1)}} \tag{7}$$

*Step 3:* (Voltage Update) Solve for $\left[V^{(m)}\right]$ in (6) using forward/backward substitution.

*Step 4:* (Convergence Test) Check if the power mismatch values (8), evaluated using the most recently available voltage and current, are within tolerance for all trains:

$$\left|(V_k^{(m)} - V_g^{(m)})I_k^{(m)} - P_{Tk}\right| \leq \varepsilon \tag{8}$$

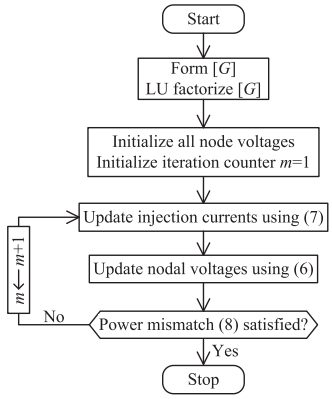


Fig. 4. Flowchart of the CI power flow.

If the convergence test is satisfied, stop and print the solution, otherwise go to *Step 2*.

A flowchart of the CI power flow is given in Fig. 4.

## III. Regenerative Trains and Nonreversible Substations

Voltage rise in DC traction networks is associated with the operation of regenerative braking systems and gets more pronounced when the supply is non-receptive, i.e when the supply is incapable of absorbing the regenerated power and presents a high resistance to the train [24]. In practice, the rise in voltage is brought under control via a chopper-controlled rheostatic brake. This section presents a two-phase approach to simulate the local control of voltage in the CI method (Section II). Phase-1 (Section III-A) is a sensitivity method to efficiently simulate the adjustment of regenerative power that is fed to the network, when interleaved with the CI power flow iterations. Phase-2 (Section III-B) employs the phase-1 solution to compute the resistance of each regenerating train; it then proceeds with the solution of the network having non-receptive substations via the CI method but with the regenerating trains represented using a voltage-current source model.

### A. Regenerative Trains (Phase-1)

The trains operating in the regenerative braking mode increase the catenary voltage while supplying their braking power to the network. If the catenary voltage of any regenerating train exceeds the prescribed limit, the regenerated power that is returned to the network must be reduced to bring the voltage within its maximum limit via squeeze control [5], [13]; this is achieved by means of a local controller that dissipates part of the regenerated power in braking resistors [24]. Cai et al. model the behavior of the local controller in power flow through successive power reduction, i.e. the power supplied by the regenerating train is gradually reduced until the right power balance is found and the train voltage is at its limit [5]. Although this approach is effective in controlling voltage, it may require a large number of CI iterations to achieve power balance.

The alternative technique presented herein is a sensitivity matrix approach for simultaneously adjusting the power injected

Authorized licensed use limited to: American University of Beirut. Downloaded on May 08,2024 at 05:24:30 UTC from IEEE Xplore. Restrictions apply.

into the network from all regenerating trains with over-voltage. Consider for illustration that the trains connected at catenary nodes $c1, \ldots, j, k, \ldots, cn$ are operating in regenerative braking mode and have higher than the prescribed voltage limit ($V_j^{\max}$); the corresponding sensitivity matrix equation is given by:

$$[H]\,[\Delta P_T] = [\Delta V] \tag{9}$$

$$[H] = \begin{bmatrix} \frac{\partial V_{c1}}{\partial P_{Tc1}} & \cdots & \frac{\partial V_{c1}}{\partial P_{Tj}} & \frac{\partial V_{c1}}{\partial P_{Tk}} & \cdots & \frac{\partial V_{c1}}{\partial P_{Tcn}} \\ \vdots & \ddots & \vdots & \vdots & \ddots & \vdots \\ \frac{\partial V_j}{\partial P_{Tc1}} & \cdots & \frac{\partial V_j}{\partial P_{Tj}} & \frac{\partial V_j}{\partial P_{Tk}} & \cdots & \frac{\partial V_j}{\partial P_{Tcn}} \\ \frac{\partial V_k}{\partial P_{Tc1}} & \cdots & \frac{\partial V_k}{\partial P_{Tj}} & \frac{\partial V_k}{\partial P_{Tk}} & \cdots & \frac{\partial V_k}{\partial P_{Tcn}} \\ \vdots & \ddots & \vdots & \vdots & \ddots & \vdots \\ \frac{\partial V_{cn}}{\partial P_{Tc1}} & \cdots & \frac{\partial V_{cn}}{\partial P_{Tj}} & \frac{\partial V_{cn}}{\partial P_{Tk}} & \cdots & \frac{\partial V_{cn}}{\partial P_{Tcn}} \end{bmatrix} \tag{10}$$

$$[\Delta P_T] = \begin{bmatrix} \Delta P_{Tc1} \\ \vdots \\ \Delta P_{Tj} \\ \Delta P_{Tk} \\ \vdots \\ \Delta P_{Tcn} \end{bmatrix}, \quad [\Delta V] = \begin{bmatrix} \Delta V_{c1} \\ \vdots \\ \Delta V_j \\ \Delta V_k \\ \vdots \\ \Delta V_{cn} \end{bmatrix} \tag{11}$$

The elements of the voltage correction vector $[\Delta V]$ are given by

$$\Delta V_j = V_j^{\max} - V_j^{(m)},\ j = c1, \ldots, cn \tag{12}$$

where $V_j^{(m)}$ is the voltage solution from the CI algorithm. The vector $[\Delta P_T]$ is obtained by solving the linear system in (9), and is used to update the regenerative power that gets injected into the network according to:

$$P_{Tj} = P_{Tj}^{(m)} + \Delta P_{Tj},\ j = c1, \ldots, cn \tag{13}$$

where $P_{Tj}^{(m)}$ denotes the train power injection used in the last CI solution; note that if $P_{Tj}$ falls outside its limit values, then it is clamped at the violated limit. In summary, when a stable voltage solution is obtained from the CI method, the catenary voltages of the regenerative trains are first checked to see if they violate their maximum prescribed limits. If there are violated voltages, the sensitivity matrix (9) is solved to update the train powers employed in the next iteration of the CI algorithm, which is initialized using the last voltage solution. The iterations between the CI voltage update and the sensitivity computation/current update are continued until a stable voltage solution is found that (i) satisfies the train power mismatch (8) and (ii) does not violate any voltage limit on regenerating trains. The implementation of

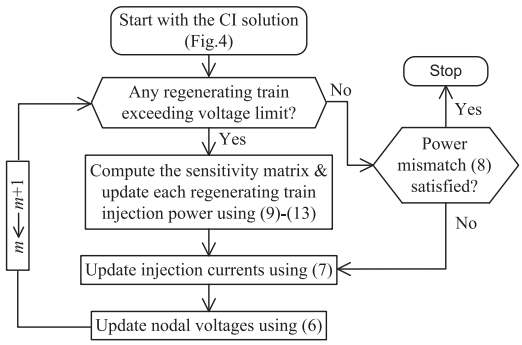


Fig. 5. Flowchart of the phase-1 solution.

the sensitivity based CI method requires the following change to steps 2-4 in Section II, starting from a CI solution:

*Step 2:* (Sensitivity Computation/Current Update) For regenerating trains that exceed the prescribed voltage limit, adjust the train injection powers using (9)-(13). Increment the iteration counter $m$ by 1 and compute the node current injection vector $\left[I^{(m)}\right]$ using (7).

*Step 3:* (Voltage Update) Solve for $\left[V^{(m)}\right]$ in (6) using forward/backward substitution.

*Step 4:* (Convergence Test) Check if all regenerative train voltages do not exceed their prescribed limits by $\varepsilon_V$, and if the power mismatch values (8) are within tolerance $\varepsilon$ for all trains. If the convergence test is satisfied, stop and print the solution, otherwise go to *Step 2*.

A similar procedure is implemented to restrict the power consumed by motoring trains whenever their catenary voltage drops below a prescribed minimum value. Fig. 5 shows a flowchart of the phase-1 solution.

*1) Sensitivity Matrix:* The sensitivity analysis requires the computation of the partial derivatives in (10). Towards this end, the modified conductance matrix in (6) is inverted to express the nodal voltages in function of the injection currents via a modified resistance matrix:

$$\begin{bmatrix} V_1 \\ \vdots \\ V_k \\ V_g \\ \vdots \\ V_N \end{bmatrix} = \begin{bmatrix} R_{11} & \cdots & R_{1k} & R_{1g} & \cdots & R_{1N} \\ \vdots & \ddots & \vdots & \vdots & \ddots & \vdots \\ R_{k1} & \cdots & R_{kk} & R_{kg} & \cdots & R_{kN} \\ R_{g1} & \cdots & R_{gk} & R_{gg} & \cdots & R_{gN} \\ \vdots & \ddots & \vdots & \vdots & \ddots & \vdots \\ R_{N1} & \cdots & R_{Nk} & R_{Ng} & \cdots & R_{NN} \end{bmatrix} \begin{bmatrix} V_s \\ \vdots \\ I_k \\ I_g \\ \vdots \\ 0 \end{bmatrix} \tag{14}$$

To compute a sensitivity element on the diagonal of $[H]$, for instance $\frac{\partial V_k}{\partial P_{Tk}}$, consider only the injection currents that are related to $P_{Tk}$ as being nonzero:

$$I_k = \frac{P_{Tk}}{V_k - V_g},\ I_g = \frac{-P_{Tk}}{V_k - V_g} \tag{15}$$

The voltages $V_k$ and $V_g$ at the catenary and track connection nodes become:

$$V_k = (R_{k1} + \cdots)\, V_s + (R_{kk} - R_{kg})\, \frac{P_{Tk}}{V_k - V_g} \tag{16}$$

Authorized licensed use limited to: American University of Beirut. Downloaded on May 08,2024 at 05:24:30 UTC from IEEE Xplore. Restrictions apply.

$$V_g = (R_{g1} + \cdots) V_s + (R_{gk} - R_{gg}) \frac{P_{Tk}}{V_k - V_g} \quad (17)$$

Taking the derivative of (16), (17) with respect to $P_{Tk}$, and making use of the chain-rule, gives:

$$\begin{bmatrix} A & B \\ C & D \end{bmatrix} \begin{bmatrix} \dfrac{\partial V_k}{\partial P_{Tk}} \\ \dfrac{\partial V_g}{\partial P_{Tk}} \end{bmatrix} = \begin{bmatrix} \dfrac{R_{kk} - R_{kg}}{V_k - V_g} \\ \dfrac{R_{gk} - R_{gg}}{V_k - V_g} \end{bmatrix} \quad (18)$$

where

$$A = 1 + \frac{R_{kk} - R_{kg}}{(V_k - V_g)^2} P_{Tk},\ B = \frac{R_{kg} - R_{kk}}{(V_k - V_g)^2} P_{Tk} \quad (19)$$

$$C = \frac{R_{gk} - R_{gg}}{(V_k - V_g)^2} P_{Tk},\ D = 1 - \frac{R_{gk} - R_{gg}}{(V_k - V_g)^2} P_{Tk} \quad (20)$$

The solution to (18) gives the sensitivity coefficients:

$$\frac{\partial V_k}{\partial P_{Tk}} = \frac{(R_{kk} - R_{kg})(V_k - V_g)}{(V_k - V_g)^2 + P_{Tk}(R_{kk} + R_{gg} - R_{kg} - R_{gk})} \quad (21)$$

$$\frac{\partial V_g}{\partial P_{Tk}} = \frac{(R_{gk} - R_{gg})(V_k - V_g)}{(V_k - V_g)^2 + P_{Tk}(R_{kk} + R_{gg} - R_{kg} - R_{gk})} \quad (22)$$

To compute an off-diagonal sensitivity element in $[H]$, for instance $\frac{\partial V_j}{\partial P_{Tk}}$, consider:

$$V_j = (R_{j1} + \cdots) V_s + (R_{jk} - R_{jg}) \frac{P_{Tk}}{V_k - V_g} \quad (23)$$

The derivate of $V_j$ with respect to $P_{Tk}$, is obtained from (23) using the chain-rule:

$$\frac{\partial V_j}{\partial P_{Tk}} = \frac{R_{jk} - R_{jg}}{V_k - V_g} - \frac{R_{jk} - R_{jg}}{(V_k - V_g)^2} P_{Tk} \left( \frac{\partial V_k}{\partial P_{Tk}} - \frac{\partial V_g}{\partial P_{Tk}} \right) \quad (24)$$

Substituting (21) and (22) in (24) gives:

$$\frac{\partial V_j}{\partial P_{Tk}} = \frac{(R_{jk} - R_{jg})(V_k - V_g)}{(V_k - V_g)^2 + P_{Tk}(R_{kk} + R_{gg} - R_{kg} - R_{gk})} \quad (25)$$

### *B. Nonreversible Substations (Phase-2)*

Even if all the regenerative train power injections are reduced to prevent any voltages exceeding their limits, the regenerated power returned to the network may still be greater than the total motoring power. This will cause power to flow back into the supply through some or all of the substations; while this may be possible with inverting substations [18]–[20], it is not realistic with nonreversible substations as the rectifiers become reverse biased. Nonreversible substations are commonly available in practical DC traction systems, and this makes it necessary to account for them in the power flow solution.

One approach is to check the substation power after a voltage solution is obtained. If reverse power is found to be flowing through a substation, the substation is turned off and a new stable voltage solution is sought via the CI method. A problem arises when all the substations are turned off; in this case the power flow solution with all trains modeled as current sources cannot be reliably computed, due to the absence of any slack power source. The regenerative train model in Fig. 6 is used to circumvent this problem: whenever one or more substations are turned off, the regenerating trains are converted into a voltage source in series with a resistance connected to node $k$, and a current source $I_k$ (equal to the current supplied by the regenerative train) connected to node $g$. The voltage source is set to the maximum allowed catenary voltage $V_k^{\max}$ and the resistance $R_k$ is chosen according to:

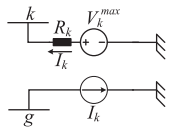


Fig. 6. Voltage-current source regenerative train model.

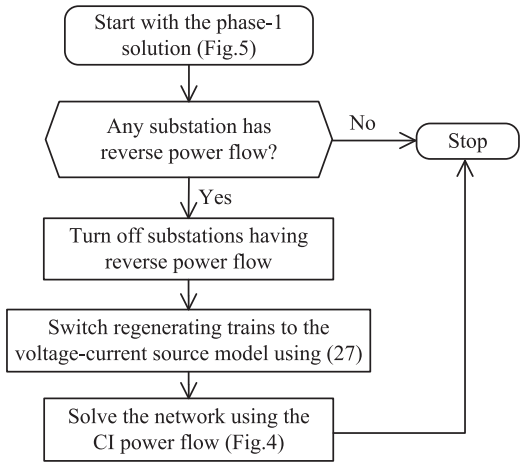


Fig. 7. Flowchart of the phase-2 solution.

$$I_k = \frac{P_{Tk}}{V_k - V_g} = \frac{V_k^{\max} - V_k}{R_k} \quad (26)$$

$$\Rightarrow R_k = \frac{(V_k^{\max} - V_k)(V_k - V_g)}{P_{Tk}} \quad (27)$$

The choice of $R_k$ according to (27) is such that when none of the substations are turned off, then the CI voltage solution with all trains modeled as current sources (Fig. 2) will also be a solution to the network with the regenerative trains represented as in Fig. 6. This is evident because for the same voltage solution, (26) stipulates that the regenerative train injection currents are identical when using the models from Figs. 2 and 6. Consequently when any of the substations having reverse power flow is turned off, the regenerative trains will have to supply less current to the network. This results in less voltage drop over $R_k$ and therefore a higher catenary voltage; this voltage cannot however exceed the maximum prescribed value $V_k^{\max}$, which is chosen as the voltage source value in Fig. 6. A flowchart of the phase-2 solution is given in Fig. 7.

Authorized licensed use limited to: American University of Beirut. Downloaded on May 08,2024 at 05:24:30 UTC from IEEE Xplore. Restrictions apply.

TABLE I
COMPARATIVE PERFORMANCE RESULTS FOR THE NETWORK WITH 18 TRAINS

| Case # | Proposed PF | | Ref. [5] | | SUF |
|---|---|---|---|---|---|
| iter. | time [ms] | iter. | time [ms] | | |
| 0 | 43 | 148 | 43 | 148 | 1.0 |
| 1 | 38 | 147 | 38 | 147 | 1.0 |
| 2 | 32 | 148 | 32 | 148 | 1.0 |
| 3 | 25 | 150 | 25 | 145 | 1.0 |
| 4 | 17 | 145 | 17 | 145 | 1.0 |
| 5 | 16 | 145 | 16 | 145 | 1.0 |
| 6 | 16 | 145 | 16 | 145 | 1.0 |
| 7 | 15 | 146 | 15 | 146 | 1.0 |
| 8 | 26 | 163 | 52 | 165 | 1.0 |
| 9 | 28 | 164 | 1275 | 244 | 1.5 |
| 10 | 24 | 165 | 1777 | 291 | 1.8 |
| 11 | 26 | 166 | 2632 | 382 | 2.3 |
| 12 | 26 | 166 | 4239 | 528 | 3.2 |
| 13 | 28 | 166 | 5956 | 687 | 4.1 |
| 14 | 27 | 166 | 6275 | 729 | 4.4 |
| 15 | 27 | 166 | 7436 | 840 | 5.1 |
| 16 | 27 | 167 | 8816 | 960 | 5.8 |
| 17 | 25 | 166 | 9744 | 1049 | 6.3 |
| 18 | 26 | 166 | 11299 | 1196 | 7.2 |

TABLE II
TRAIN POWER FOR CASE # 9 ( IN KW - ACTIVE SIGN CONVENTION)

| Train # | Reversible SS | | Nonreversible SS | |
|---|---|---|---|---|
| Proposed | [5] | Proposed | [5] | |
| 1 | 75.75 | 76 | 47.84 | 48.07 |
| 2 | 150 | 150 | 95.39 | 95.56 |
| 3 | 126.18 | 126 | 105.49 | 105.38 |
| 4 | 150 | 150 | 147.40 | 147.40 |
| 5 | 150 | 150 | 147.80 | 147.80 |
| 6 | 150 | 150 | 149.25 | 149.25 |
| 7 | 150 | 150 | 148.32 | 148.32 |
| 8 | 150 | 150 | 149.16 | 149.16 |
| 9 | 71.76 | 71 | 45.32 | 44.91 |
| 10 | −150 | −150 | −150 | −150 |
| 11 | −150 | −150 | −150 | −150 |
| 12 | −150 | −150 | −150 | −150 |
| 13 | −150 | −150 | −150 | −150 |
| 14 | −150 | −150 | −150 | −150 |
| 15 | −150 | −150 | −150 | −150 |
| 16 | −150 | −150 | −150 | −150 |
| 17 | −150 | −150 | −150 | −150 |
| 18 | −150 | −150 | −150 | −150 |

TABLE III
CATENARY VOLTAGES FOR CASE # 9 ( IN V )

| Train # | Reversible SS | | Nonreversible SS | |
|---|---|---|---|---|
| | Proposed | [5] | Proposed | [5] |
| 1 | 787.50 | 787.40 | 787.50 | 787.44 |
| 2 | 773.95 | 773.91 | 778.94 | 778.90 |
| 3 | 787.50 | 787.44 | 787.50 | 787.45 |
| 4 | 746.95 | 746.93 | 747.68 | 747.66 |
| 5 | 742.86 | 742.85 | 743.55 | 743.53 |
| 6 | 746.02 | 746.02 | 746.23 | 746.23 |
| 7 | 774.79 | 774.78 | 774.93 | 774.92 |
| 8 | 758.70 | 758.70 | 758.86 | 758.85 |
| 9 | 787.50 | 787.32 | 787.50 | 787.39 |
| 10 | 687.94 | 687.91 | 696.97 | 696.93 |
| 11 | 676.93 | 676.91 | 679.74 | 679.71 |
| 12 | 668.64 | 668.62 | 669.93 | 669.91 |
| 13 | 664.23 | 664.22 | 665.27 | 665.25 |
| 14 | 718.90 | 718.89 | 719.21 | 719.21 |
| 15 | 702.50 | 702.50 | 702.79 | 702.78 |
| 16 | 659.86 | 659.85 | 662.83 | 662.81 |
| 17 | 697.54 | 697.54 | 698.83 | 698.82 |
| 18 | 713.04 | 713.03 | 713.31 | 713.30 |

## IV. NUMERICAL RESULTS

The CI power flow method (Section II) and the two-phase approach (Section III) were programmed in Matlab. The programs were run on an iMAC having a 2.7 GHz quad-core Intel Core i5 processor with 4 MB L3 cache and 8 GB of RAM. The parameters employed in the stopping criteria are $\varepsilon = 0.0001$ W in the CI method and $\varepsilon_V = 0.0001$ V for checking the maximum permissible catenary voltage violations.

### *A. Benchmark Test Network With 18 Trains*

The benchmark test network consists of a double track 750 V DC traction system whose diagram and data are available in [1], [2], [25]; the upper permissible catenary voltage is set to 787.5 V. The system has 3 substations and 18 trains, and an upper track and a lower track each having a branch. The ground network is represented using the finite cell model with a cell defined for each 100 m of the track length. This gives a DC power flow problem with 779 nodes. Nineteen simulation cases were studied, with case #0 having all trains in motoring mode, case #1 having the first train in regenerative braking mode and the remaining ones in motoring mode, case #2 having the first 2 trains in regenerative braking mode and the remaining ones in motoring mode, etc. Table I shows for each case the CI iterations and the execution time using the proposed sensitivity based CI method (phase-1). The proposed method was compared with the power reduction and balance method in [5], and the computational performance results are given in columns 4 and 5 in Table I. It is evident that the proposed method and that in [5] are identical up to case #7, as there is no requirement to reduce the regenerated power that is fed in the network due to over-voltage. The situation changes in cases #8 to #18, where it is seen that [5] requires a large number of power reduction steps with the increasing number of regenerating trains; on the other hand, the sensitivity method maintains roughly the same number of CI iterations and computing time. The speed-up factor (SUF = time of the method in [5]/time of the sensitivity method), which is given in column 6 of Table I, increases to around 7 as the number of regenerating trains increases. Notably, the proposed approach maintains convergence within 26 CI iterations even for the extreme case #18 in which all trains are in regenerative braking mode.

Tables II and III show representative comparative results of the train power and catenary voltages for case #9. The results in column 2 of Tables II and III reveal that the sensitivity method reduced the power of the regenerating trains #1, #3, and #9 from 150 kW to satisfy the permissible pantograph voltage limit. The computation of the substations' power, as given in Table IV,

Authorized licensed use limited to: American University of Beirut. Downloaded on May 08,2024 at 05:24:30 UTC from IEEE Xplore. Restrictions apply.

TABLE IV
SUBSTATION VOLTAGE, CURRENT, AND OUTPUT POWER FOR CASE # 9 (PHASE-1: REVERSIBLE SUBSTATIONS)

| Node # | Positive [V] | Negative [V] | Current [A] | Power [kW] |
|---|---|---|---|---|
| 25 | 750.55 | 0.55 | −176.93 | −132.70 |
| 26 | 741.62 | −8.38 | 400.07 | 300.05 |
| 27 | 744.27 | −5.73 | 229.40 | 172.05 |

TABLE V
SUBSTATION VOLTAGE, CURRENT, AND OUTPUT POWER FOR CASE # 9 (PHASE-2: NONREVERSIBLE SUBSTATIONS)

| Node # | Positive [V] | Negative [V] | Current [A] | Power [kW] |
|---|---|---|---|---|
| 25 | 766.40 | −4.27 | 0 | 0 |
| 26 | 741.91 | −8.09 | 398.17 | 298.63 |
| 27 | 744.61 | −5.39 | 224.25 | 168.18 |

shows that the substation at node #25 is conducting power to the AC network side. Given that such a situation is not permissible for nonreversible substations, the computation proceeds to phase-2 in which the substation is blocked and the regenerating trains are switched to the voltage-current source model in Fig. 6; the resistance in Fig. 6 is held constant at the value given by (27). Column 4 in Table II gives the train power from the CI method with the regenerating trains switched to their voltage-current source model (phase-2), and Table V shows that the substation at node #25 is now no longer conducting power. Columns 3 and 5 in Tables II and III present the power flow results using the method in [5]; a power reduction step of 1 kW is employed to get results comparable in accuracy to those obtained from the sensitivity method. The results show that the proposed method gives results almost identical to [5], with the minor differences attributed to using a fixed power reduction step. Note that none of the catenary voltages in Table III exceed the set limit of 787.5 V, and the voltages corresponding to motoring trains are substantially lower but still above the 650 V limit stipulated in [13]; while it is possible to reduce the power drawn by motoring trains to raise the lower voltage values in a scheme quite similar to squeeze control [13], networks such as the Swedish railway locomotive system will still remain in operation for voltage drops of around 40% [6].

### B. Larger Test Networks

The proposed method was also contrasted with [5] on larger test instances with 36, 72, and 144 trains. These test instances were formed starting from the typical parameter values and structure of the traction network in [1], [2]. Table VI shows the number of trains, the number of substations, and the total number of nodes (including ground circuit modeling) in the three networks; the electronic companion [25] includes schematics of the network interconnections and the complete data sets. The traction systems were simulated under three scenarios involving 50%, around 75%, and 100% of the trains in regenerative braking mode. The required CI iterations and computing time are

TABLE VI
MAIN CHARACTERISTICS OF THE LARGER TEST NETWORKS

| Trains ($N_T$) | Substations ($N_S$) | Nodes ($N$) |
|---|---|---|
| 36 | 6 | 1558 |
| 72 | 12 | 3116 |
| 144 | 24 | 6304 |

TABLE VII
COMPARATIVE PERFORMANCE RESULTS FOR THE LARGER TEST NETWORKS

| | Reg. | Proposed PF | | Ref. [5] | | SUF |
|---|---|---|---|---|---|---|
| Trains | Trains | iter. | time [ms] | iter. | time [ms] | |
| 36 | 18 | 32 | 170 | 2420 | 466 | 2.7 |
| 36 | 28 | 29 | 174 | 13733 | 2065 | 11.8 |
| 36 | 36 | 26 | 177 | 22216 | 3301 | 18.7 |
| 72 | 36 | 32 | 188 | 4090 | 1244 | 6.6 |
| 72 | 56 | 29 | 207 | 27070 | 7529 | 36.5 |
| 72 | 72 | 26 | 214 | 44228 | 12288 | 57.4 |
| 144 | 72 | 32 | 346 | 8104 | 4001 | 11.6 |
| 144 | 112 | 29 | 410 | 53557 | 25679 | 62.7 |
| 144 | 144 | 26 | 430 | 87718 | 42116 | 98.0 |

presented in Table VII. It is noticed that the computational performance of the competing power reduction and balance method [5] deteriorates at a fast pace, with both the increasing number of trains and their proportion in regenerative braking mode; this is contrary to the performance of the proposed method where the computing time remains within 0.5 s even for the network with 144 regenerating trains. The speed-up factor (SUF in the last column of Table VII) shows that the computational advantage of the proposed technique relative to [5] increases with system size and with the number of regenerating trains to reach around 98.

## V. CONCLUSION

This paper presented a two-phase approach for simulating local controllers in DC traction power flow applications that model limited network receptivity. The approach builds on the commonly adopted CI power flow technique. Phase-1 is a sensitivity method for adjusting the regenerated power that is fed back to the network in blended regenerative/rheostatic braking; the power adjustment is computed to keep the catenary voltages within their permissible limits, but assumes that the stations are reversible. Phase-2 accounts for limited network receptivity due to nonreversible substations; this is achieved in the CI method by switching each of the regenerating trains to a voltage-current source model whose resistance value is computed from the voltage solution in phase-1 without iteration, in contrast to [5]. Numerical results show that the sensitivity based CI method obviates the need for many of the power reduction steps in [5], and gives a speed-up factor that significantly increases with the network size and the number of regenerating trains.

Authorized licensed use limited to: American University of Beirut. Downloaded on May 08,2024 at 05:24:30 UTC from IEEE Xplore. Restrictions apply.

## REFERENCES


[1] R. J. Hill and Y. Cai, "Simulation of rail voltage and earth current in a PC-based traction power simulator," *WIT Trans. Eng. Sci.*, vol. 3, pp. 1–8, 1993.

[2] R. J. Hill and Y. Cai, "An efficient computational technique for a DC rail traction power flow simulator incorporating track branches," *WIT Trans. Model. Simul.*, vol. 5, pp. 1–12, 1993.

[3] S. N. Talukdar and R. L. Koo, "The analysis of electrified ground transportation networks," *IEEE Trans. Power App. Syst.*, vol. PAS-96, no. 1, pp. 240–247, Jan. 1977.

[4] T. Kulworawanichpong, "Multi-train modeling and simulation integrated with traction power supply solver using simplified Newton-Raphson method," *J. Mod. Transp.*, vol. 23, no. 4, pp. 241–251, 2015.

[5] Y. Cai, M. R. Irving, and S. H. Case, "Iterative techniques for the solution of complex dc-rail-traction systems including regenerative braking," *IEE Proc., Gener. Transm. Distrib.*, vol. 142, no. 5, pp. 445–452, Sep. 1995.

[6] L. Abrahamsson and L. Söder, "Fast estimation of relations between aggregated train power system data and traffic performance," *IEEE Trans. Veh. Technol.*, vol. 60, no. 1, pp. 16–29, Jan. 2011.

[7] L. Abrahamsson, T. Kjellqvist, and S. Östlund, "High-voltage DC-feeder solution for electric railways," *IET Power Electron.*, vol. 5, no. 9, pp. 1776–1784, Nov. 2012.

[8] R. J. Hill, Y. Cai, S. H. Case, and M. R. Irving, "Discussion of: Iterative techniques for the solution of complex DC-rail-traction systems including regenerative braking," *IEE Proc., Gener. Transm. Distrib.*, vol. 143, no. 6, pp. 613–615, Nov. 1996.

[9] J. G. Yu and C. J. Goodman, "Modelling of rail potential rise and leakage current in DC rail transit systems," in *Proc. IEE Colloq. Stray Current Effects DC Railways Tramways*, Oct. 1990, pp. 2/2/1–2/2/6.

[10] Y. Cai, M. R. Irving, and S. H. Case, "Modelling and numerical solution of multibranched DC rail traction power systems," *IEE Proc., Elect. Power Appl.*, vol. 142, no. 5, pp. 323–328, Sep. 1995.

[11] C. L. Pires, S. I. Nabeta, and J. R. Cardoso, "ICCG method applied to solve DC traction load flow including earthing models," *IET Elect. Power Appl.*, vol. 1, no. 2, pp. 193–198, Mar. 2007.

[12] M. Coto, P. Arboleya, and C. Gonzalez-Moran, "Optimization approach to unified AC/DC power flow applied to traction systems with catenary voltage constraints," *Int. J. Elect. Power Energy Syst.*, vol. 53, pp. 434–441, 2013.

[13] P. Arboleya, B. Mohamed, C. González-Morán, and I. El-Sayed, "BFS algorithm for voltage-constrained meshed DC traction networks with non-smooth voltage-dependent loads and generators," *IEEE Trans. Power Syst.*, vol. 31, no. 2, pp. 1526–1536, Mar. 2016.

[14] C. L. Pires, S. I. Nabeta, and J. R. Cardoso, "DC traction load flow including AC distribution network," *IET Elect. Power Appl.*, vol. 3, no. 4, pp. 289–297, Jul. 2009.

[15] P. Arboleya, G. Diaz, and M. Coto, "Unified AC/DC power flow for traction systems: A new concept," *IEEE Trans. Veh. Technol.*, vol. 61, no. 6, pp. 2421–2430, Jul. 2012.

[16] P. Arboleya, M. Coto, C. González-Morán, and R. Arregui, "On board accumulator model for power flow studies in DC traction networks," *Elect. Power Syst. Res.*, vol. 116, pp. 266–275, Nov. 2014.

[17] Z. Jia, Z. Yang, F. Lin, and X. Fang, "Dynamic simulation of the DC traction power system considering energy storage devices," in *Proc. IEEE Conf. Expo. Transp. ElectrificAsia-Pac., (ITEC Asia-Pacific)*, Aug. 2014, pp. 1–6.

[18] T. Suzuki, "DC power-supply system with inverting substations for traction systems using regenerative brakes," *IEE Proc. B, Elect. Power Appl.*, vol. 129, no. 1, pp. 18–26, Jan. 1982.

[19] B. Mellitt, Z. S. Mouneimne, and C. J. Goodman, "Simulation study of DC transit systems with inverting substations," *IEE Proc. B, Elect. Power Appl.*, vol. 131, no. 2, pp. 38–50, Mar. 1984.

[20] D. Cornic, "Efficient recovery of braking energy through a reversible DC substation," in *Proc. Elect. Syst. Aircraft, Railway Ship Propulsion*, Oct. 2010, pp. 1–9.

[21] I. Džafić, H.-T. Neisius, M. Gilles, S. Henselmeyer, and V. Landerberger, "Three-phase power flow in distribution networks using Fortescue transformation," *IEEE Trans. Power Syst.*, vol. 28, no. 2, pp. 1027–1034, May 2013.

[22] I. Džafić, B. C. Pal, M. Gilles, and S. Henselmeyer, "Generalized $\pi$ Fortescue equivalent admittance matrix approach to power flow solution," *IEEE Trans. Power Syst.*, vol. 29, no. 1, pp. 193–202, Jan. 2014.

[23] J. D. Irwin and R. M. Nelms, *Basic Engineering Circuit Analysis*, 9th ed. Hoboken, NJ, USA: Wiley, 2008.

[24] R. G. Fletcher, "Regenerative equipment for railway rolling stock," *Power Eng. J.*, vol. 5, no. 3, pp. 105–114, May 1991.

[25] DC railway traction network data sets. [Online]. Available: https://www.dropbox.com/s/hqtx6stfaj5tk5s/DC_Railway_Net.zip?dl=0. Accessed on: Mar. 25, 2017.



**Rabih A. Jabr** (M'02–SM'09–F'16) was born in Lebanon. He received the B.E. degree in electrical engineering (with high distinction) from the American University of Beirut, Beirut, Lebanon, in 1997, and the Ph.D. degree in electrical engineering from Imperial College London, London, U.K., in 2000. He is currently a Professor in the Department of Electrical and Computer Engineering, American University of Beirut. His research interests are in mathematical optimization techniques and power system analysis and computing.

**Izudin Džafić** (M'05–SM'13) received the Ph.D. degree from the University of Zagreb, Zagreb, Croatia, in 2002. He is currently an Associate Professor in the Department of Electrical Engineering, International University of Sarajevo, Bosnia. From 2002 to 2014, he was with Siemens AG, Nuremberg, Germany, where he held the position of the Head of the Department and Chief Product Owner (CPO) for Distribution Network Analysis (DNA) R&D. His research interests include power system modeling, and development and application of fast computing to power systems simulations.

Dr. Džafić is a member of the IEEE Power and Energy Society and the IEEE Computer Society.


Authorized licensed use limited to: American University of Beirut. Downloaded on May 08,2024 at 05:24:30 UTC from IEEE Xplore. Restrictions apply.